

Electron-hole bilayer quantum dots: Phase diagram and exciton localization

K. Kärkkäinen^a M. Koskinen^a M. Manninen^a S.M. Reimann^b

^a*Department of Physics, University of Jyväskylä, FIN-40014, Finland*

^b*Mathematical Physics, Lund Institute of Technology, P.O. Box 118, S-22100 Lund, Sweden*

Abstract

We studied a vertical “quantum dot molecule”, where one of the dots is occupied with electrons and the other with holes. We find that different phases occur in the ground state, depending on the carrier density and the interdot distance. When the system is dominated by shell structure, orbital degeneracies can be removed either by Hund’s rule, or by Jahn-Teller deformation. Both mechanisms can lead to a maximum of the addition energy at mid-shell. At low densities and large interdot distances, bound electron-hole pairs are formed.

Key words: Quantum dot molecule, Electron-hole plasma

PACS: 73.21.La, 71.35.Ee, 73.21.-b

Semiconductor quantum dots share many qualities with natural atoms, and are thus often referred to as “artificial atoms” (for reviews see [1,2]). In single quantum dots, shell structure could be observed [3]: large differences in the addition energies occurred at particular electron numbers ($N = 2, 6, 12$) corresponding to closed shells, forming the “quantum dot noble gases”. Just like in real atoms, for half-filled shells spin alignment due to Hund’s rule leads to an increased stability of the system [3,4]. Quantum dots are uniquely suited to explore regimes of many-electron systems that are not accessible in conventional atomic physics, and much fundamental new insight on correlated states in these low-dimensional many-body systems was gained in the past years.

Quantum dot artificial atoms can be coupled to form “artificial molecules”. Such systems have been studied much both experimentally [5] and theoretically [6], and were even discussed in connection with potential quantum computing devices [7]. Most work focused on vertically or laterally coupled double quantum dots with electrons. More recently, Anisimovas and Peeters [8,9] examined the correlated few-particle states in a vertical *bipolar* quantum dot

molecule, consisting of two vertically coupled quantum dots, one populated by electrons, the other by holes. They applied the exact diagonalization method in the limit of a strong, spin-polarizing magnetic field [8] and furthermore studied the dynamic response within a hydrodynamic model [9]. The experimental realization of such electron-hole double quantum dots should for example be possible in bilayer-bipolar heterostructures with separated electron- and hole layers in equilibrium, as in biased GaAs/AlGaAs or InAs/GaSb [10]. These bipolar systems have attracted much attention recently, last but not least due to the exciting possibility of making a Bose-Einstein condensate with indirect excitons [11]. The phases of a symmetric electron-hole bilayer system were recently also investigated by Liu *et al.* [12], and by Paolo *et al.* [13] in the fixed-node diffusion Monte Carlo approach [14] with periodic boundary conditions.

In this Communication, we demonstrate that small bipolar-bilayer systems consisting of only a few electrons and holes show a very rich phase diagram which in fact appears to be different from the “bulk” [13]: depending on the electron- and hole-densities and the interdot distance, the ground state is either dominated by shell structure, leading to a competition between Jahn-Teller deformation [15] and spin alignment in the case of orbital degeneracies, or by the formation of localized, bound electron-hole pairs (“localized excitons”).

As schematically sketched in the inset to Fig. 1, a quantum dot with electrons in one (two-dimensional) layer is separated by a distance z_0 from a quantum dot confining holes in the other 2D layer. The charge carriers in both layers are confined by a harmonic potential, $V = m_{e,h}^* \omega_0^2 r^2 / 2$, with $r^2 = x^2 + y^2$ (a model which is frequently applied to describe single quantum dots [16,17]). The two layers are electrostatically coupled with no interdot tunneling, i.e., recombination is prohibited.

To obtain the ground state energies and densities, we apply the density functional method in the local spin density approximation [18]. For the bipolar bilayer system, we have to solve four coupled equations for the electron- and hole spin densities, $n_{\uparrow}^e(\mathbf{r}), n_{\downarrow}^e(\mathbf{r})$ and $n_{\uparrow}^h(\mathbf{r}), n_{\downarrow}^h(\mathbf{r})$. For electrons and holes, respectively, the effective Kohn-Sham potential $v_{\text{eff}}^{e(h)\sigma}(\mathbf{r})$ consists of the external harmonic confinement, the electron-electron (hole-hole) repulsion, the electron-hole (hole-electron) attraction and the exchange-correlation potential v_{xc}^{σ} which is approximated in the local spin-density approximation. We use the von Barth and Hedin [19] formulation of the local electron (hole) exchange-correlation energy $\varepsilon_{xc}(n^{e(h)}, \zeta^{e(h)}) = \varepsilon_{xc}(n^{e(h)}, 0) + f(\zeta^{e(h)})[\varepsilon_{xc}(n^{e(h)}, 1) - \varepsilon_{xc}(n^{e(h)}, 0)]$, where $\zeta^{e(h)}$ is the electron (hole) spin polarization and $f(\zeta^{e(h)}) = ((1 + \zeta^{e(h)})^{3/2} + (1 - \zeta^{e(h)})^{3/2} - 2)/(2^{3/2} - 2)$ is the polarization dependence. The function $f(\zeta^{e(h)})$ interpolates between the paramagnetic ($\zeta^{e(h)} = 0$) and ferromagnetic ($\zeta^{e(h)} = 1$) cases given by Tanatar and Ceperley [20]. The electron-

hole correlation is neglected. This is a good approximation for large interdot separation (the correlation energy is then diminished) and for strong external confinement (the correlation energy is then small compared to the kinetic and exchange energies). Even in the equilibrium density of the electron hole plasma the correlation energy is much smaller than the exchange energy [21] (the equilibrium density minimizes the total energy of the two-dimensional plasma in an infinite system).

For example, the Kohn-Sham single particle wave functions for the electrons in one of the two dots, $\psi_{i\sigma}^e(\mathbf{r})$, satisfy the Kohn-Sham equations with the effective potential for the electrons, given by

$$v_{\text{eff}}^{e\sigma}(\mathbf{r}) = \frac{1}{2}m^*\omega_0^2r^2 + v_{xc}^\sigma(n^e(\mathbf{r}), \zeta^e(\mathbf{r})) + \int \frac{n^e(\mathbf{r}')}{|\mathbf{r} - \mathbf{r}'|} d\mathbf{r}' - \int \frac{n^h(\mathbf{r}')}{\sqrt{|\mathbf{r} - \mathbf{r}'|^2 + z_0^2}} d\mathbf{r}'. \quad (1)$$

The electron density $n^e(\mathbf{r})$ in Eq. 1 is given by

$$n^e(\mathbf{r}) = \sum_{i,\sigma} |\psi_{i\sigma}^e(\mathbf{r})|^2, \quad (2)$$

where σ corresponds to the two spins $\sigma = (\downarrow, \uparrow)$ and i refers to the lowest occupied states. A corresponding relation holds for the hole density $n^h(\mathbf{r})$ in the other dot. $\zeta^e(\mathbf{r})$ is the spin polarization for electrons, $\zeta^e(\mathbf{r}) = (n_\uparrow^e(\mathbf{r}) - n_\downarrow^e(\mathbf{r}))/n^e(\mathbf{r})$. The Kohn-Sham equations for electrons and holes were solved self-consistently using a plane wave technique applied earlier to single dots [22,4]. No symmetry restrictions for the charge or spin densities were applied.

For simplicity, let us assume equal effective masses of electrons and holes, $m_e^* = m_h^* = m^*$, and also restrict the numbers of electrons and holes confined in each of the wells to be equal, $N_e = N_h = N$. (Throughout the paper, we use effective atomic units with the energy measured in effective Hartree, $\text{Ha}^* = m^*e^4/\hbar^2(4\pi\epsilon_0\epsilon)^2$ and the distance in effective Bohr radii, $a_B^* = \hbar^2(4\pi\epsilon_0\epsilon)/m^*e^2$. With the effective mass m^* and dielectric constant ϵ , the results then scale to the value of the semiconductor material in question.) The vertical double dot is then described by three parameters: the distance between the dots z_0 , the strength of the confining potential ω_0 (taken to be equal for both dots), and the number of electrons and holes. Due to the attractive interactions between the electrons and holes and since we assumed that $N_e = N_h = N$, the obtained ground state electron density necessarily equals that of the holes, $n^e(\mathbf{r}) = n^h(\mathbf{r})$; in the z -direction the densities are of course separated by z_0 . The spin density of the electrons and holes are also equal, but the relative direction of the electron and hole spins is not determined since there is no

direct spin-spin interaction.

In the phase space determined by z_0 and ω_0 three limiting cases are of particular interest:

(i) If both z_0 and ω_0 are zero, the limit of the two-dimensional electron-hole plasma is reached. The average density for large N will approach the equilibrium density of the plasma. In the case of small droplets, for non-closed shells the orbital degeneracies are removed by internal Jahn-Teller deformation of the density, resulting in intriguing geometries of the ground state densities. This regime was called earlier the “ultimate jellium” limit, and has also been studied in connection with the physics of simple metal clusters [23] both in the two-dimensional [22] and in the three-dimensional case [24,25].

(ii) When ω_0 is still zero (or very small), but z_0 becomes larger, the average particle density in each dot decreases and eventually, the particles begin to localize in a lattice. In comparison to the formation of “Wigner-molecules” in quantum dots with electrons [26], here the localization is clearly seen also in the local density approximation due to the attractive interaction between the electrons and the holes: they localize on top of each other forming a lattice of bound electron-hole pairs (“localized excitons”). Since the electrons and holes are confined in different layers, these electron-hole pairs have electric dipole moments and consequently repel each other. In each dot the localized electrons (or holes) show antiferromagnetic order (i.e., the so-called “spin density wave” [27,28,29]) in the ground state. The formation of bound electron-hole pairs is somewhat similar to the states discussed by Anisimovas and Peeters [8] for strong interdot coupling in a polarizing magnetic field.

(iii) When ω_0 increases the strong confinement eventually hinders the internal deformation and the electron and hole densities are forced to be azimuthally symmetric. The degeneracy in an open-shell dot can then be reduced by magnetization according to Hund’s first rule [3,4].

Figure 1 shows the phase diagram of the $N = 4$ system. This case is particularly interesting since for a single dot, the second shell is half-filled having two p -electrons and spin $S = 1$ [4]. In the limit of the “ultimate jellium” ($z_0 = 0$, $\omega_0 = 0$), on the other hand, the system is strongly deformed and non-magnetic. Figure 1 shows the regions of different magnetic and geometrical structures in the z_0 - ω_0 -plane. It is interesting to note that for small interdot distances the deformed system is the ground state up to a large value of ω_0 (for $z_0 = 0$ the circular $S = 1$ state becomes the ground state when $\hbar\omega_0 > 1.3 \text{ Ha}^*$). For small values of ω_0 we see a transition from the deformed state to the state with localized excitons when z_0 increases.

A single dot with $N = 6$ has a filled electronic shell and naturally $S = 0$. Nevertheless, for a very weak confinement the ground state shows a spin-

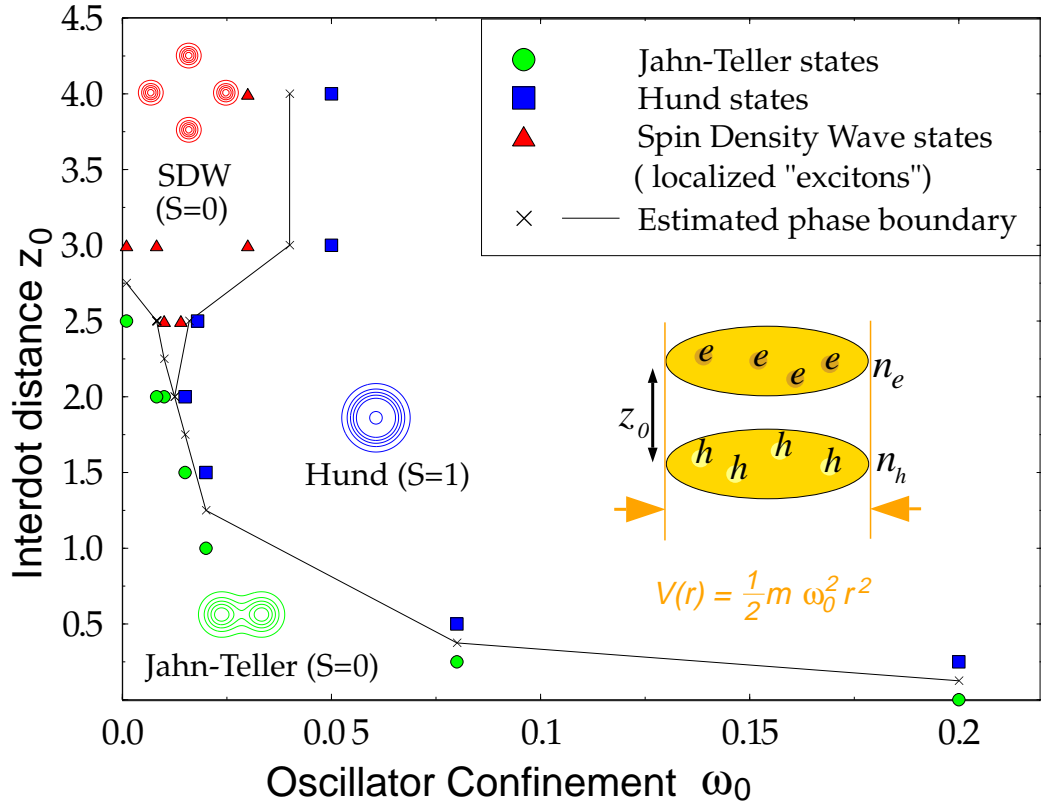


Fig. 1. Phase diagram of an electron-hole double dot with 4 electrons and 4 holes. ω_0 is the strength of the external confinement and z_0 the interdot distance (in atomic units). The dashed lines show the estimated phase boundaries separating different spin-structures. The characteristic particle density is shown for each phase. The squares (spin $S = 1$) and triangles ($S = 0$) indicate the calculated points which are closest to the estimated phase boundaries. *Inset to the right:* Schematic picture of the bipolar quantum dot molecule with electrons (e) and holes (h) harmonically confined in two layers, which are separated by a distance z_0 .

density wave [4]. A similar behavior is obtained for the electron-hole double dot at large values of the interdot distance z_0 . In the limit of small external confinement, the ground state appears to be a hexagon of localized excitons. Classically, a more favorable geometry would be a pentagon with one exciton at the center. However, in this case the hexagon is favored due to the formation of a spin-density wave, i.e., antiferromagnetic order of the spins in each dot (a centered pentagon would lead to “frustration”). The ground state of the $N = 6$ double dot in the limit of the “ultimate jellium” ($\omega_0 = 0, z_0 = 0$) does not have azimuthal symmetry, but is triangular, which seems to be the dominating geometry for closed-shell electron-hole clusters in two dimensions [22,30]. The phase diagram (not printed here) shows a transition from a nonmagnetic triangular density to circular density when ω_0 increases, and to localized electrons with a spin density wave when z_0 increases (for small ω_0).

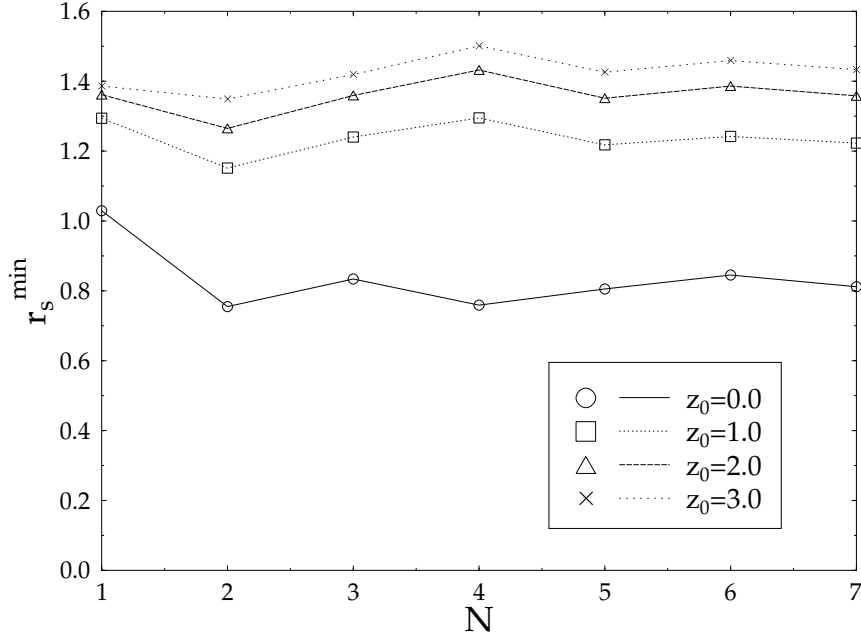


Fig. 2. Minimum of the *local* r_s as a function of the number N of electrons and holes for different values of the interdot distance z_0 . The average carrier density of a single dot was kept approximately independent of N (see text).

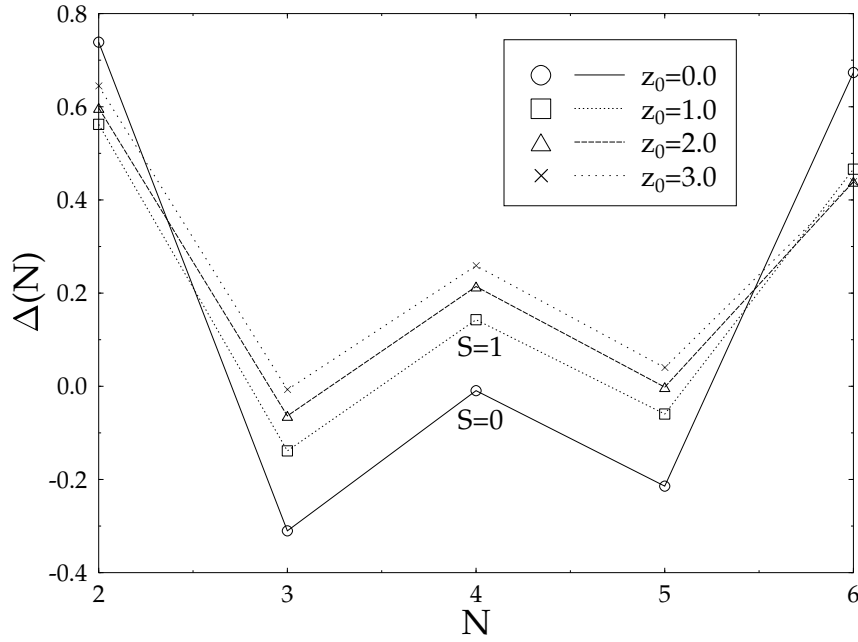


Fig. 3. The addition energy spectrum for different values of z_0 . The average carrier density of a single dot was kept approximately independent of N (see text).

In the above phase diagram, the number of electrons and holes N was fixed. When N is varied, however, experimental data on single quantum dots suggest [2] to keep the *average* density in each dot constant. This can be achieved by the relation $\omega_0^2(N) = e^2/(4\pi\epsilon\epsilon_0 m^* r_s^3 \sqrt{N})$ (see Ref. [4]). The parameter $r_s = 1/\sqrt{\pi n}$ measures the in-layer coupling strength and is defined in terms of the in-layer areal density $n^{e(h)}(\mathbf{r})$ for the electrons and holes, respectively. Here, we use the r_s -value corresponding to the equilibrium density of the two-dimensional electron gas ($r_s = 1.51 a_B^*$). Neglecting the electron-hole correlation, this density is also the equilibrium density of the electron-hole plasma without external confinement.

In the double dot system a single dot corresponds to the limit of infinite z_0 . When the interdot distance decreases, the electron-hole attraction increases the effective confinement and the density increases slightly. However, since the r_s -value has been chosen to be at the equilibrium density of the electron-hole plasma, $r_s = 1.5 a_B^*$, this effect is small. Figure 2 shows the minimum *local* value of r_s (determined from the maximum density) obtained in the dots for different values of N and z_0 , using the above relation for $\omega_0(N)$. For $z_0 = 3 a_B^*$ the minimum r_s is already close to $1.5 a_B^*$ for all values of N . The variation as a function of N is caused by the shell structure: The smallest value is obtained for the closed shell system, $N = 2$, and the maximum value for the half-filled shell $N = 4$. The lowest curve ($z_0 = 0$) corresponds to the situation where the deformation wins against Hund's rule, leading to a different dependence of the minimum r_s on N .

In the case of single quantum dots the *addition energy spectrum* gives information about the shell structure. Maxima in the addition energy differences were observed for closed shells, and at mid-shell spin alignment due to Hund's rule leads to enhanced stability [3]. For the bipolar bilayer system studied here, we find that intriguingly, the addition energy spectra also reveal the internal Jahn-Teller deformation of the system. The difference in the electrochemical potentials of a bipolar double dot confining $(N+1)$ and N electrons *and holes* is given by $\Delta(N) = E(N+1) - 2E(N) + E(N-1)$, i.e., the second differences of the corresponding total ground state energies $E(N)$.

Figure 3 shows the addition energy differences $\Delta(N)$ for $z_0 \leq 3 a_B^*$. The addition energy maxima for the closed shells at $N = 2$ and $N = 6$ can be clearly seen. An additional maximum occurs at mid-shell, $N = 4$. It is interesting to note that also the case $z_0 = 0$ shows a similar spectrum. In this case the maximum at $N = 4$ is not caused by Hund's rule, but by the Jahn-Teller deformation, which is strongest at half-filled shells.

In conclusion, we have studied symmetric vertical electron-hole double dots using the geometrically unrestricted spin-density functional method. In the limit of small distances between the dots, the effective confinement is gov-

erned by the electron-hole electrostatic attraction and the properties of the system are determined by the Jahn-Teller deformation of the particle densities. In the limit of weak external confinement, at increasing interdot distance electrons and holes form separate “excitons” which localize forming a lattice with antiferromagnetic spin-coupling in each dot. When the external confinement becomes large, Hund’s rule determines the spin in each dot. The addition energy spectrum shows a maximum at half-shell. At large interdot distances this maximum is caused by Hund’s rule while at small distances the maximum is a result of the Jahn-Teller deformation of the particle density.

This work has been supported by the Academy of Finland under the Finnish Centre of Excellence Programme 2000-2005 (Project No. 44875, Nuclear and Condensed Matter Programme at JYFL), NORDITA, the Swedish Research Foundation (VR) and the Swedish Foundation for Strategic Research (SSF).

References

- [1] T. Chakraborty, *Quantum Dots: A Survey of the Properties of Artificial Atoms* (North-Holland, Amsterdam 1999).
- [2] S.M. Reimann and M. Manninen, Rev. Mod. Phys. **74**, 1283 (2002).
- [3] S. Tarucha et. al., Phys. Rev. Lett. **77**, 3613 (1996).
- [4] M. Koskinen, S.M. Reimann, and M. Manninen, Phys. Rev. Lett. **79**, 1389 (1997).
- [5] F.R. Waugh *et al.*, Phys. Rev. Lett. **75**, 705 (1995); F. Hofmann *et al.*, Phys. Rev. B **51**, 13872 (1995); D. Dixon *et al.*, Phys. Rev. B **53**, 12625 (1996); R.H. Blick *et al.*, Phys. Rev. B **53**, 7899 (1996), Phys. Rev. Lett. **80**, 4032 (1998); *ibid.* **81**, 689 (1998); G. Schedelbeck *et al.*, Science **278**, 1792 (1997); D.G. Austing *et al.*, Semicond. Sci. Technol. **12**, 631 (1997), Jap. J. Appl. Phys. **36**, 1667 (1997), Physica B **249-251**, 206 (1998); T. Schmidt *et al.*, Phys. Rev. Lett. **78**, 1544 (1997); T.H. Oosterkamp *et al.*, Science **278**, 1792 (1997), Phys. Rev. Lett. **80**, 4951 (1998), Nature **395**, 873 (1998); A. Lorke and R.J. Luyken, Physica B **256-258**, 424 (1998); M. Brodsky *et al.*, Phys. Rev. Lett. **85**, 2356 (2000); M. Bayer *et al.*, Science **291**, 451 (2001).
- [6] J.J. Palacios and P. Hawrylak, Phys. Rev. B **51**, 1769 (1995); H. Imamura, P.A. Maksym and H. Aoki, Phys. Rev. B **53**, 12613 (1996), *ibid.* **59**, 5817 (1999); M. Rontani *et al.*, Solid State Commun. **112**, 151 (1999), *ibid.* **119**, 309 (2001); C. Yannouleas and U. Landman, Phys. Rev. Lett. **82**, 5325 (1999), (E) *ibid.* **85**, 2220 (2000); J. Kolehmainen *et al.*, Eur. Phys. J. B **13** 731 (2000); B. Partoens and F.M. Peeters, Phys. Rev. Lett. **84**, 4433 (2000); A. Wensauer *et al.*, Phys. Rev. B **62**, 2605 (2000); L. Martin-Moreno *et al.*, Phys. Rev. B **62**, R10633 (2000); M. Pi et al., Phys. Rev. B **57**, 14783 (2001), Phys. Rev. Lett. **87**, 066801 (2001).

- [7] D. Loss and D.P. Di Vincenzo, Phys. Rev. A **57**, 120 (1998); G. Burkhard, D. Loss, and D.P. Di Vincenzo, Phys. Rev. B **59**, 2070 (1999).
- [8] E. Anisimovas and F.M. Peeters, Phys. Rev. B **65**, 233302 (2002).
- [9] E. Anisimovas and F.M. Peeters, Phys. Rev. B **66**, 075311 (2002).
- [10] U. Sivan, P.M. Solomon, and H. Shtrikman, Phys. Rev. Lett. **68**, 1196 (1992); T.P. Marlow *et al.*, Phys. Rev. Lett. **82**, 2362 (1999); J. Kono *et al.*, Phys. Rev. B **55**, 1617 (1997).
- [11] L.V. Butov *et al.*, Nature **417**, 47 (2002).
- [12] L. Liu, L. Świerkowski, D. Neilson, and J. Szymański, Phys. Rev. B **53**, 7923 (1996).
- [13] S. De Paolo, F. Rapisarda, and G. Senatore, Phys. Rev. Lett. **88**, 206401 (2002).
- [14] *Quantum Monte Carlo Methods in Physics and Chemistry*, ed. M.P.Nightingale and C. Umrigar, Kluwer, Dordrecht, 1999.
- [15] H.A. Jahn and E. Teller, Proc. R. Soc. London A **161**, 220 (1937).
- [16] V. Shikin *et al.*, Phys. Rev. B **43**, 11903 (1991).
- [17] A. Kumar, S.E. Laux and F. Stern, Phys. Rev. B **42**, 5166 (1990).
- [18] W. Kohn, and L.J. Sham, Phys. Rev. **140**, A1133 (1965).
- [19] U. von Barth and L. Hedin, J. Phys. C **5**, 1629 (1972).
- [20] B. Tanatar and D.M. Ceperley, Phys. Rev. B **39**, 5005 (1989).
- [21] W.F. Brinkman and T.M. Rice, Phys. Rev. B **7**, 1508 (1973); P. Vashishta and R.K. Kalia, Phys. Rev. B **23**, 6492 (1982).
- [22] S.M. Reimann, M. Koskinen, J. Helgesson, P.E. Lindelof, and M. Manninen, Phys. Rev. B **58**, 8111 (1998).
- [23] W. de Heer, Rev. Mod. Phys. **65**, 611 (1993); M. Brack, Rev. Mod. Phys. **65**, 677 (1993).
- [24] M. Manninen, Phys. Rev. B **34**, 6886 (1986).
- [25] M. Koskinen, P.O. Lipas, and M. Manninen, Z. Phys. D **35**, 285 (1995).
- [26] Yu. E. Lozovik, and V.A. Mandelshtam, Phys. Lett. A **145**, 269 (1990), Phys. Lett. A **165**, 469 (1992); F. Bolton and U. Rössler, Superlatt. Microstr. **13**, 139 (1993); Bedanov, V.M., and F.M. Peeters, Phys. Rev. B **49**, 2667 (1994).
- [27] S.M. Reimann, M. Koskinen, M. Manninen, Phys. Rev. B **59**, 1613 (1999).
- [28] M. Koskinen, M. Manninen, S.M. Reimann, B. Mottelson, Phys. Rev. B **63**, 205323 (2001).

- [29] M. Manninen, M. Koskinen, S.M. Reimann, B. Mottelson, Eur. Phys. J. D **16**, 381 (2001).
- [30] S.M. Reimann, M. Koskinen, H. Häkkinen, P.E. Lindelof, and M. Manninen, Phys. Rev. B **56**, 12147 (1997).